Microbial Dysbiosis Associated with Impaired Intestinal Na+/H+ Exchange Accelerates and Exacerbates Colitis in Ex-Germ Free Mice

Christy A. Harrison[1,2], **Daniel Laubitz**[1], **Christina L. Ohland**[3], **Monica T. Midura-Kiela**[1], **Karuna Patil**[3], **David G. Besselsen**[3], **Deepa R. Jamwal**[1], **Christian Jobin**[4,*], **Fayez K. Ghishan**[1,*], and **Pawel R. Kiela**[1,2,*]

[1]Department of Pediatrics, Steele Children's Research Center, Tucson Arizona, United States of America

[2]Department of Immunobiology, University of Arizona College of Medicine, Tucson, Arizona, United States of America

[3]University Animal Care, University of Arizona, Tucson, Arizona, United States of America

[4]Department of Medicine, Division of Gastroenterology, University of Florida College of Medicine, Gainesville, Florida, United States of America

Abstract

Intestinal epithelial Na^+/H^+ exchange facilitated by the apical NHE3 (*Slc9a3*) is a highly-regulated process inhibited by intestinal pathogens and in inflammatory bowel diseases. $NHE3^{-/-}$ mice develop spontaneous, bacterially-mediated colitis, and IBD-like dysbiosis. Disruption of epithelial Na^+/H^+ exchange in IBD may thus represent a host response contributing to the altered gut microbial ecology, and may play a pivotal role in modulating the severity of inflammation in a microbiome-dependent manner. To test whether microbiome fostered in an NHE3-deficient environment is able to drive mucosal immune responses affecting the onset or severity of colitis, we performed a series of cohousing experiments and fecal microbiome transplants into germ-free Rag-deficient or $IL-10^{-/-}$ mice. We determined that in the settings where the microbiome of NHE3-deficient mice was stably engrafted in the recipient host, it was able accelerate the onset and amplify severity of experimental colitis. NHE3-deficiency was characterized by the reduction in pH-sensitive butyrate-producing *Firmicutes* families *Lachnospiraceae* and *Ruminococcaceae*

Correspondence: Pawel R. Kiela, DVM, PhD, *University of Arizona, Steele Children's Research Center,* 1501 N. Campbell Ave, Rm. 6351, Tucson, AZ 85724. Fax: (520) 626-4141; Ph: (520) 626-9687; pkiela@peds.arizona.edu.
*Shared senior authorship

Disclosures: All authors declare that there is no conflict of interest to disclose

(Clostridia clusters IV and XIVa), with an expansion of inflammation-associated *Bacteroidaceae*. We conclude that the microbiome fostered by impaired epithelial Na^+/H^+ exchange enhances the onset and severity of colitis through disruption of the gut microbial ecology.

INTRODUCTION

The intestinal epithelium is the first innate barrier that protects from luminal commensal and pathogenic microbiota, and actively contributes to the development and function of the mucosal immune system. Several genetic IBD susceptibility loci have been linked to genes with critical roles in the epithelial cell function, and functional dynamic changes in tight junction maintenance, mucus and antimicrobial peptide secretion, endoplasmic reticulum (ER) stress, and insufficient autophagy.[1] One of the primary roles of epithelial cells, nutrient transport, has been known to be affected by the inflammatory process. Changes in membrane transport have been considered responsible for secondary symptoms such as nutritional deficiencies or inflammation-associated diarrhea, and not as primary contributors to the disease process. This view is gradually changing as we begin to understand the consequences of altered epithelial transport to the mucosal and systemic homeostasis, gut microbiome, and to the local inflammatory process itself.[2]

Apical Na^+/H^+ exchange at the brush border of the absorptive gut epithelia serves several purposes, all critical to maintaining mucosal homeostasis. It is the key contributor to transepithelial Na^+ and water absorption, provides acidic milieu at the brush border to support nutrient transport by providing an inwardly directed proton gradient utilized for short-chain fatty acid (SCFA) absorption, supports low pH needed to maintain a compact and impenetrable inner mucus layer, couples functionally with glucose and bicarbonate transport, and regulates intracellular pH.[3, 4] NHE3, the product of the *Slc9a3* gene, is considered to be the dominant isoform of the three apically expressed Na^+/H^+ exchangers (NHE2, 3, and 8).[5] Pro-inflammatory cytokines such as interferon gamma (IFNγ) and tumor necrosis factor alpha (TNFα) reduce NHE3 expression and activity[6–8], a phenomenon also prominently observed *in vivo* in several models of experimental colitis[9–11], and in IBD patients.[11–14] NHE3 is also inhibited by bacterial toxins produced by *Vibrio cholerae*[15] or *Clostridium difficile*[16], and by enteropathogenic *E. coli* via a mechanism depending on the type III secretion system and EspF.[17] Since gel-forming mucins produced by goblet and epithelial cells require acidic pH to maintain their compacted concatenated ring structures[18], disruption of NHE3 and the ensuing elevated pH of the inner mucus layer is likely responsible for the observed increased penetration and eventually bacterial translocation to the lamina propria,[19] and stimulation of local immune response. Indeed, NHE3-deficient mice develop spontaneous colitis with features characteristic of human IBD.[20] Their resting mucosal IFNγ production is elevated with increased numbers of CD8α^+ T cells and NK cells as the main source of the cytokine in the intraepithelial and lamina propria compartments, and are dramatically susceptible to DSS-induced mucosal injury.[21] Spontaneous colitis could be completely ameliorated and the response to DSS delayed by the administration of broad-spectrum antibiotics,[20, 21] collectively providing strong evidence for the necessary role for the gut microbiome in the development of disease in this model. Moreover, NHE3-deficient mice develop a dramatic dysbiosis, reminiscent in some ways of

the changes described among IBD patients.[22] These observations in the colon were further strengthened by an independent report by Engevik et al.[23] who reported ileal expansion of *Bacteroides thetaiotaomicron* in NHE3^{−/−} mice, a verified colitogenic pathobiont.[24, 25] NHE3-status was the defining and dominant factor in driving dysbiosis in adoptively transferred NHE3/Rag2 double-knockout mice, a model characterized by dramatically accelerated and exacerbated progression of colitis.[26]

Current dogma holds that the immune system develops an aberrant and progressive overreaction to commensal microbes, leading to host-damaging autoimmune disease. However, until recently it was unclear whether the microbiome in IBD is causative or merely reflective of disease. Limited published data support the notion that a dysbiotic microbiome can either transfer susceptibility[27] or outright transmit colitis.[28] In this report, we hypothesized that loss of NHE3 mediates the onset of colitis by shaping the microbiota. Thus, we sought to determine if the dysbiotic microbiota developed from NHE3 deficiency is sufficient alone to transmit susceptibility to experimental colitis in an NHE3-sufficient host. We tested this via cohousing under specific-pathogen free (SPF) conditions, fecal microbiome transplant (FMT) into germ-free (GF) Rag1^{−/−} mice followed by adoptive T cell transfer, and FMT into GF IL10^{−/−} mice. Dysbiosis was stably maintained only in IL10^{−/−} FMT recipients, a model known for the inhibition of the endogenous NHE3.[10] In this host, significant reductions of butyrate-producing *Firmicutes* families *Lachnospiraceae* and *Ruminococcaceae* and an expansion of *Bacteroidaceae* correlated with earlier onset and increased colitis severity. These observations provide evidence that disruption of the intestinal Na^+/H^+ exchange during inflammation results in a microbial environment fostering mucosal inflammatory responses.

RESULTS

Dysbiotic microbiome or susceptibility to T cell-mediated colitis are not transferred from NHE3^{−/−} to wild-type (WT) mice via passive microbiome sharing

Microbiome is a vital part of the pathogenesis of colitis associated with the loss of NHE3. Cohousing was chosen as the first approach to address the question whether microbial dysbiosis precipitated by NHE3 deficiency is dominant, passively transferrable, and sufficient to transmit susceptibility to experimental T cell-mediated colitis. All mice were raised and maintained in an ultraclean barrier facility (see description in the Methods section). Rag2^{−/−} (Rag) mice were co-housed with either NHE3xRag2^{−/−} double knockout (DKO) mice in a ratio of 2:3 Rag:DKO, or with other Rag mice as a control (Fig. S1A). As coprophagic animals, mice continually share their microbiome by consuming their own and their cage-mates' fecal pellets.[29] Cohousing has been demonstrated in several studies as efficient means of horizontal microbial transfer, with some inherent limitations.[30] After a week of cohousing to normalize the microbiome in resting conditions, Rag mice were adoptively transferred with 5×10^5 flow-sorted naïve CD4^{+}CD45RB[HI] T cells. Control Rag mice were injected with sterile PBS as baseline controls. Experimental Rag mice (2 per cage, 6 per group) that had been housed with either Rag or DKO cage-mates were adoptively transferred with T cells. Fecal samples were collected from untreated Rag and DKO cage-mates to monitor the comparative microbiota of each genotype (Fig. 1A). Cage-mates were

maintained in the cage to share living quarters and continuously donate fecal matter, but not otherwise studied. All adoptively transferred animals were Rag mice (Fig. S1A). The study continued for 8 weeks post-T cell transfer with weekly longitudinal fecal pellet collection for microbiome study. Comparison of alpha diversity and composition between groups suggested that the microbiome from DKO mice was not stably established in their cage-mates via horizontal transfer (Fig. 1B and 1C). Despite the dramatically lower alpha diversity of DKO donor mice, Rag mice cohoused with either Rag or DKO mice had a comparable alpha diversity (Fig. 1B). This suggested that the dysbiotic microbiome associated with NHE3-deficiency could not compete by passive exposure in a stable NHE3-competent host. Regardless of the co-housed fecal donors, adoptive transfer with T cells was associated with reductions in the *Lachnospiraceae* family, especially the *Roseburia* genus, and a reciprocal expansion of *Bacteroidaceae* (Fig. 1C and S2), most likely co-occurring with the onset of inflammation.

Despite the failure to gain weight (Fig. 1D), adoptively transferred Rag mice housed with DKO mice did not have significant evidence of enhanced hyperplasia (Fig. 1E) or colonic inflammation (Fig. 1F and S3A) in comparison to Rag mice cohoused with NHE3-competent mice. The colonic mucosa also showed no significant evidence of enhanced expression of inflammatory cytokines by qPCR (Fig. S3B). Thus, lack of passive microbiome sharing between DKO and Rag knockout mice in the cohousing study corresponded with no detectable aggravation of colitis in response to adoptive T cell transfer.

Direct fecal microbiome transplant stably introduces microbial communities from NHE3 sufficient and deficient donors into germ-free mice

We next performed Fecal Microbial Transplant (FMT) from Rag control or DKO fecal donors into germ-free recipients (Fig. S1B). As proof of principle, we first established that the respective microbial communities could be stably transplanted into wildtype germ-free recipients using oral inoculation. Fecal samples were collected weekly post-association for nine weeks to monitor the microbiome composition. Although DKO fecal donors lacking endogenous NHE3 expression had a more dramatically dysbiotic microbiome composition and lower diversity than the wild-type GF recipients of DKO FMT (Fig. 1A, 2A, and S4A), unweighted Unifrac analysis clearly indicated that different microbiome communities from Rag and DKO mice could be stably introduced to wildtype GF mice (Fig. 2B). While weighted analysis showed that there was some convergence over time in the microbiome (Fig. 2C), taxonomic analysis of individual mice indicated that the major phyla (Fig. 2D) and most bacterial families (Fig. S4B) remained stably different over the course of the nine weeks. The only major exception was the *Bacteroidaceae* family (Fig. 2E), which steadily declined in the wildtype recipients of DKO FMT to eventually reach nearly normal levels observed in the recipients of the control FMT. This observation suggested that perhaps this bacterial family is competitive in the colonic microenvironment fostered in DKO mice, but not under healthy wildtype conditions. Wildtype recipients of FMT from DKO had reduced alpha diversity as compared to the recipients of FMT from control Rag mice (Fig. 2A).

Temporal dynamics and convergence of microbiomes in ex-germ free (ex-GF) Rag mice corresponds with limited pro-inflammatory effect of FMT from NHE3-deficient donors

Having confirmed an efficient establishment of Rag and DKO microbiomes in germ-free wild-type mice, we aimed to determine whether we could reproduce the susceptibility to T-cell mediated colitis we recently reported in adoptively-transferred DKO mice[26] using microbiome transplant alone, using germ-free (GF) Rag1$^{-/-}$ mice colonized with the dysbiotic microbiota from DKO mice (Fig. S1C). Fresh fecal samples were collected from 4–6 Rag or DKO mice and pooled within each genotype. Fecal slurries were then used to inoculate GF Rag1$^{-/-}$ mice. Germ-free mice that have subsequently been inoculated with microbiota are referred to in this article as ex-germ-free (ex-GF). Following a week of equilibration after inoculation, 5×10^5 of naïve CD4$^+$CD45RB^{HI} T cells were adoptively transferred via i.p. injection to induce colitis. Mice were sacrificed 4.5 weeks post-T cell transfer due to veterinary concern regarding stool consistency and weight loss in selected animals. Beta diversity analysis of the longitudinally collected samples showed that although the DKO FMT recipients' microbiomes remained in a stable dysbiotic state, the T-cell transferred recipients of FMT from control Rag mice began to converge over time toward the dysbiotic DKO microbiome, likely as a result of developing colitis (Fig. 3A). This was most prominent for the major phyla *Bacteroidetes* and *Firmicutes* (Fig. 3B), and driven at the family level by dramatic reductions in SCFA-producing *Firmicutes* families *Lachnospiraceae* and *Ruminococcaceae*, as well as reductions in *Clostridiales vadinBB60*, and a relative expansion of *Bacteroidaceae* (Fig. 3C). Alpha diversity trended lower in recipients of the DKO microbiome, albeit to a lesser extent compared to donors or in the initial experiment with FMT into wildtype GF recipients (Fig. 3D).

Consistent with the convergence of the microbiomes over time, endpoint analysis of colitis at 4.5 weeks after T cell transfer showed only mildly enhanced inflammation in the recipients of DKO microbiome, as compared to the FMT from healthy Rag (Fig. 4 and 5). GF Rag mice that had received FMT from DKO initially lost weight but regained it by the termination of the experiment (Fig. 4A) and showed a trend towards increased colonic hyperplasia as expressed by colonic weight/length ratio (Fig. 4B). Histology and pathological interpretation indicated that the recipients of FMT from DKO mice had similar trends towards elevated inflammation scores in both proximal and distal colon, however without reaching statistical significance (p~0.08 for each measure; Fig. 4D–F). Mucosal IL1β was significantly elevated in the recipients of DKO FMT, while expression of TNF, IL-12p40, MMP8 (neutrophil collagenase; surrogate marker of neutrophilic infiltration), and iNOS followed similar trends without reaching statistical significance (Fig. 5A–E).

Immunofluorescence staining for the neutrophil marker Ly6B.2 indicated a significantly elevated influx of neutrophils in the distal colon of DKO microbiota recipients compared to recipients of FMT from Rag mice (Fig. 5F and 5G). There was significantly higher influx of CD4$^+$ cells in the proximal colon, and a positive trend in the distal colon of DKO FMT recipients (Fig. 5F and 5H). Together, these indicate that recipients of the microbiota from DKO mice had a heightened immune response and influx of inflammatory immune cells. Immunofluorescence for cleaved caspase 3 to measure apoptotic cells also indicated a trend toward more cleaved caspase 3 positive cells in the distal colon by cell count, and a

significant elevation of staining intensity from cleaved caspase 3 in both segments (Fig. 5F, 5I, and 5J), indicating greater levels of apoptosis among recipients of DKO microbiota.

In conclusion, adoptive naïve T cell transfer into GF Rag1$^{-/-}$ mice associated with Rag or DKO microbiomes showed that DKO microbiome remained in a stable dysbiotic state, whereas the recipients of "healthy" microbiomes of NHE3-competent donors converged over time to resemble aspects of the NHE3$^{-/-}$-like "inflammatory" dysbiosis. This was driven by dramatic reductions in several anti-inflammatory *Firmicutes* families and a reciprocal expansion of *Bacteroidaceae*, which on a genus level was entirely accounted for by *Bacteroides* (data not shown). Modest inflammatory differences were observed between the two FMT recipients, suggesting greater inflammatory response among recipients of DKO microbiota. However, consistent with the convergence of the microbiomes over time, these differences were nuanced in nature.

The NHE3$^{-/-}$ microbiome remains stably different and promotes accelerated and exacerbated inflammation in the IL-10$^{-/-}$ model of colitis

IL-10$^{-/-}$ mice provide an alternative model of chronic immune-mediated colitis, with obligatory contribution of the microbiota.[31] Introduction of commensal enteric bacteria to germ-free IL-10$^{-/-}$ animals induces progressive colonic inflammation over the course of several weeks. Moreover, colitis in IL-10$^{-/-}$ mice is known to be associated with significant inhibition of NHE3 activity[10], which makes this host more likely to retain the dysbiotic characteristics of DKO microbiome upon colonization. We performed FMT into GF IL-10$^{-/-}$ mice using the fecal slurries from the same pool of donors collected at the same time as the previous fecal transplant experiments to maintain consistency (Fig. S1D). 16S amplicon profiling of the microbiome from IL-10$^{-/-}$ recipients of FMT revealed that in contrast to the adoptive transfer fecal microbiome transplant, the microbiomes of NHE3$^{+/+}$ (Rag) and NHE3$^{-/-}$ (DKO) donors remained stably different in relation to one another over time, although we again observed a noticeable shift in the fecal microbiome of IL10$^{-/-}$ mice receiving Rag microbiome towards convergence at week 7, the final time point (Fig. 6A). At the taxonomic level, however, we observed that although the microbiomes of both groups changed over time with the onset of disease, they were often changing in parallel (Fig. S5). Again, the onset of inflammation was accompanied in the fecal microbiome by a plummeting abundance of SCFA-producing *Lachnospiraceae, Ruminococcaceae*, and *Clostridiales vadinBB60*, and a reciprocal increase in *Bacteroidaceae* (Fig. 6B and S5). In this experiment, recipients of DKO FMT also experienced an increased relative abundance of the *Erysipelotricaceae* family, which has been associated with inflammatory processes (Fig. S5).[30]

At the final time point in the fecal microbiome collection and analysis, the recipients of DKO FMT were still characterized by contractions of overall *Firmicutes* abundance, driven specifically by reductions in *Lachnospiraceae* and *Clostridiales vadinBB60* (Fig. 6B and 6D). The control group also had a higher relative abundance of *Lactobacillaceae* (Fig. 6B and 6D), but a time course analysis suggested that this was a result of an expansion in the control FMT group, not a reduction in the DKO FMT group (Fig. S5). Inflammation was also associated with a dramatic reduction of the *Roseburia* genus, which is part of the

Lachnospiraceae family and is reduced in human ulcerative colitis[31] and Crohn's disease[32] (Fig. S5). Other reductions in *Lachnospiraceae* and *Ruminococcaceae* genera were also observed (Fig. S5). In this model, we observed a similar trend in reduced alpha diversity in the fecal microbiome of DKO FMT recipients (Fig. 6C).

Considering the consistently observed decrease in SCFA-producing bacteria in both DKO donors and the recipients of the DKO microbiome, we estimated microbial butyrate (butanoate) production using the PICRUSt analysis of function bioinformatics tool. PICRUSt estimates functional pathways utilized by the microbiome based on community profiling. When comparing an untreated donor population of Rag and DKO mice to IL-10$^{-/-}$ recipients of Rag or DKO microbiota, PICRUSt indicated significant changes in the relative abundance of OTU's associated with butyric acid metabolism (Fig. 6E). Functional profiling also indicated a reduction of OTU's associated with butyrate metabolism among Rag FMT recipients with the onset of inflammation (Fig. 5E).

16S rRNA profiling of the mucosa-adherent bacteria from proximal and distal colonic segments demonstrated that many of the microbiome differences between either Rag and DKO FMT recipients observed in fecal samples were enhanced at the level of the mucosa (Fig. 6). Since they clustered together, for clarity of Fig. 7A, proximal and distal segments are not differentiated by color. DKO FMT recipients were characterized by more dramatic relative reductions of *Firmicutes* driven almost entirely by *Lachnospiraceae* and *Ruminococcaceae* (Fig. 7B and 7C), which are both SCFA-producers and mucin-degraders, and have been shown to be especially sensitive to alkalization of the microenvironment[33]. We observed some gender effect on the mucosal microbiome of the FMT recipients, but these effects, delineated across PC3, did not correspond to inflammatory response which was driven by PC1 (Fig. 7A). While interesting for future study, we have not investigated that question more deeply here. The mucosal microbiome of IL-10$^{-/-}$ recipients of NHE3$^{-/-}$ microbiome had a more noticeable decrease in alpha diversity compared to recipients of Rag FMT (Fig. 7D), in contrast to what we observed in the fecal microbiome from the same experiment (Fig. 6C). Additional functional categories identified by PICRUSt as over- or under-represented in IL-10$^{-/-}$ recipients of Rag or DKO microbiomes are listed in Figure S5 and include modest but significant increase in OTU's associated with bacterial toxins, DNA repair, or peptidoglycan synthesis, and decrease in categories representing flagellar assembly and bacterial motility (Fig. S6).

GF IL-10$^{-/-}$ mice that had received fecal microbiome from DKO mice had accelerated and mildly exacerbated colitis as compared to those that had received the control microbiome (Fig. 8). The IL-10$^{-/-}$ mice developed severe colitis in recipients of both FMT's, but the inflammation was most severe in the proximal colon of those that received DKO FMT (Fig. 8B). Inflammation scores were not significantly different in the distal colon, though distal colon is typically affected to a lesser degree than cecum and proximal colon in this model. Since FMT recipients from both groups developed severe colitis, and the histological scoring was a point-based system based on percentages of affected segments, the saturation point for pathological scoring was reached in the proximal segment and approached in the distal colon. Thus, we also analyzed as penetrance of disease, where inflammation was expressed as the number of mice exceeding the median of control group (Rag FMT recipients). One

hundred percent of DKO FMT recipients exceeded the median of controls in the proximal colon, and the majority also scored higher in the distal colon (Fig. 8C).

To assess the dynamics of colitis development, we analyzed lipocalin 2 (LCN2 or NGAL) levels in longitudinally collected fecal samples. LCN2 is secreted by immune and epithelial cells in response to toll-like receptor (TLR) stimulation to sequester iron and limit bacterial expansion, and has been established as a reliable marker of colitis in mouse models and IBD patients.[32, 33] The increase in LCN2 expression was more rapid in IL-10$^{-/-}$ recipients of DKO FMT, being significantly expressed by 5 weeks (Fig. 8D). The group that had received control FMT began to catch up at the final collection time, which coincided with the first signs of microbiome convergence (Fig. 6A). An endoscopic analysis from the five-week time point at which the LCN2 levels were significantly different between the two FMT recipient groups showed visible evidence of inflammation in DKO FMT recipients with decreased mucosal transparency, and edema, which were not seen at this time point in the recipients of control microbiome (Fig. 8E). By the final timepoint, when LCN2 levels had caught up in the control group, immunofluorescence indicated a high influx of Ly6B.2$^+$ cells (neutrophils), CD4$^+$ cells (T cells), and cleaved caspase 3$^+$ cells and debris (apoptotic cells) in both groups (Fig. 8F). Recipients of DKO FMT trended toward a higher influx of Ly6B. 2$^+$ cells in both tissue segments, relatively equal CD4$^+$ influx, and significantly higher cleaved caspase 3 activation in the distal colon (Fig. 8F and 8G). These results suggest collectively that the microbiome of NHE3-deficient mice was able to drive a more rapid colonic inflammation in ex-GF IL-10$^{-/-}$ mice.

Together, our data suggest that the microbiota of NHE3-deficient mice has inflammatory potential in germ-free recipients under two different models of experimental colitis, and that this susceptibility is accompanied by consistent loss of SCFA-producing *Firmicutes* and expansion of *Bacteroidaceae*. This suggests a mediating role of NHE3 in shaping the microbiota, and in turn the development of colitis.

DISCUSSION

The paradigm has emerged that diversity and stability of the gut ecosystem is associated with good health, where perturbations to microbial homeostasis and losses of diversity are associated with a variety of disease processes.[36] Inflammatory bowel diseases are associated with losses in microbiome diversity, with relative expansion of *Proteobacteria* and contraction of the *Firmicutes* phylum.[37–39] These losses include butyrate-producing microbes associated with the members of the *Lachnospiraceae* and *Ruminococcaceae* families,[40,41] such as *Faecalibacterium prausnitzii*.[42,43] These changes in microbial gut ecology, frequently referred to as dysbiosis, are now widely considered as an important environmental factor contributing to the pathogenesis of IBD. The importance of dysbiosis as a causative or modulating factor of the history of the disease is still not clear, as are dietary or host-related factors that lead to instability of the gut microbiome. Our previous findings pointed at the role of impaired apical Na$^+$/H$^+$ exchange as a likely mechanism contributing to microbial dysbiosis. This membrane transport is mediated by three antiporters, NHE2, NHE3, and NHE8, with subtle differences in colonic expression pattern. The latter two are inhibited in animal models of IBD,[9–11] as well as in human patients,

[11, 34, 35] and deletion of NHE3 in mice was sufficient to lead to microbiome changes similar to that observed in human IBD,[22] microbiota-dependent spontaneous colitis,[20] and increased susceptibility to mucosal injury or T-cell mediated colitis.[21, 26] These observations prompted us to hypothesize that impaired Na^+/H^+ exchange, be it the result of initial subclinical inflammation or infection, lead to microbial dysbiosis, which in turn lowers the inflammatory threshold or otherwise modulates mucosal immune responses.

We first tested the ability of the dysbiotic microbial community to horizontally transfer into healthy $Rag2^{-/-}$ mice by co-housing them with $Rag2^{-/-}$ or DKO mice, followed by adoptive T cell transfer. In this approach, we showed that dysbiosis established in NHE3-deficient mice is not dominant and does not transfer into an NHE3-sufficient host. Consistent with this observation, we did not observe different susceptibility to adoptive T cell transfer in Rag mice co-housed with DKO mice. Using GF untreated WT mice, we were able to effectively transplant and maintain dysbiotic community from DKO mice. However, T cell transfer colitis in similarly associated Rag mice led to inflammation-induced convergence of the microbial ecology in the recipients of Rag and DKO microbiomes, and the end-point analysis of colonic inflammation showed only modest effect of the FMT, again suggesting that in a scenario where microbiome merges in the new host to represent more similar composition, the effect of FMT from NHE3-deficient donors is minor. To overcome this experimental confounder, we turned to $IL-10^{-/-}$ mice, a strain known not only for strict microbial dependence in colitis susceptibility, but also for inhibition of NHE3 activity.[10] Here, we observed accelerated disease development, with the largest difference between recipient $IL-10^{-/-}$ mice seen at 5 weeks post-colonization. This observation suggested that gut microbiome shaped by disrupted Na^+/H^+ exchange can modulate the time of disease onset and its severity. Incidentally, early and adolescent IBD was reported in a subset of patients with a rare genetic disorder, congenital sodium diarrhea, associated with inactivating mutations of NHE3.[36]

Lachnospiraceae and *Ruminococcaceae*, also commonly known as *Clostridia* clusters XIVa and IV respectively, are fairly abundant members of the normal microbiome, reaching approximately 10–20% of abundance in healthy humans where they break down indigestible carbohydrates and produce short chain fatty acids (SCFA) such as butyrate.[37] Both are negatively affected in NHE3-deficient mice, which may be correlated with decreased microbial production of SCFA's, which serve as the primary energy fuel for colonocytes and exert immunomodulatory roles in the gut mucosa. These taxa are also some of the most significantly different in the $IL-10^{-/-}$ recipients of the microbiome from NHE3-sufficient and –deficient donors. Many of these family members, notably *Roseburia* spp., which was also vulnerable to inflammation in our model, largely reside in the mucus layer of the intestine.[38] This localization may make them particularly vulnerable to microenvironmental changes brought about by disruptions in sodium hydrogen exchange. NHE3, which brings in luminal sodium in exchange for cellular hydrogen, helps facilitate a pH gradient at the brush border as protons diffuse out of the unstirred layer. This gradient is important for mucin structure, which exists in a compact impenetrable layer at the lowest pH next to the epithelia, and expands with the rising pH to form the secondary mucus layer that is widely inhabited and consumed by the microbiota.[18, 39, 40] Indeed, we and others showed that NHE3

deficiency is associated with bacterial encroachment upon the brush border membrane and increased bacterial translocation.[19, 20]

Changes in pH have also been shown to have consequences on *Lachnospiraceae* and *Ruminococcaceae* families as well as SCFA production. A change from a pH of 5.5 to 6.5 dramatically stunted both bacterial abundance as well as butyrate production – shifting instead to a peak production of propionate and an expansion of *Bacteroides*.[41]

SCFA, and especially butyrate, are potent positive regulators of NHE3 expression and activity.[42, 43] Therefore, decreased relative abundance of *Lachnospiraceae* and *Ruminococcaceae* families along with colonic SCFA production in NHE3-deficient mice suggests an existence of a positive feedback mechanism whereby butyrate producers promote stable expression and activity of NHE3, which sustains acidic mucosal milieu to sustain a competitive advantage to these and other acidophilic bacteria.

In addition to the contraction of *Lachnospiraceae* and *Ruminococcaceae*, NHE3 deficiency and inflammation are consistently associated with the expansion of *Bacteroidaceae* in our model. When sequencing resolution allowed, this expansion was determined to belong exclusively to the *Bacteroides* genera (data not shown). *Bacteroidaceae* taxa have been associated with colitis, with *Bacteroides* inducing colitis in a susceptible animal model.[24] *Bacteroidaceae* is also reported to expand following ablation of nucleotide-binding oligomerization domain-containing protein 2 (NOD2), which mediates mucosal homeostasis and is one of the major allelic mutations associated with IBD.[44] The dextran-sodium sulfate (DSS) injury model of colitis also dramatically promoted *Bacteroidaceae* family expansion. [45] The species *Bacteroides thetaiotamicron*, a known pathobiont, is reportedly expanded in NHE3$^{-/-}$ mice,[23–25] although our sequencing depth did not allow us to verify whether this species was responsible. Alongside our data, in which *Bacteroidaceae* expansion follows both NHE3 deficiency and the onset of disease, it is possible that the family is both competitive under circumstances that promote mucosal inflammation, and potentially a cause of enhanced colitis. It is therefore possible that the inflammatory potential mediated by the NHE3-deficient microbiome is not strictly due to reduced SCFA production, but also the expansion of a pathobiont which favors an inflammatory milieu. Moreover, *Bacteroidaceae* benefit from the same elevation in pH that is detrimental to *Lachnospiraceae and Ruminococcaceae*[41], suggesting a trade-off that is potentially directly mediated by NHE3.

One exceptional *Firmicute* is *Clostridium difficile*, the pathobiont responsible for the epidemic of hospital related diarrhea, which is adapted to replicate optimally at a slightly higher pH than other *Clostridia* species.[46] *C. difficile* reduces NHE3 activity,[16] and the resulting pH change may give it a competitive advantage.[46] Reciprocally, *Lachnospiraceae* alone are capable of promoting resistance to *C. difficile*,[47] perhaps by the opposing effect on pH through SCFA production. This ongoing standoff is supported by the observation that our IL-10$^{-/-}$ recipients of NHE3$^{-/-}$ FMT had an expansion of *Peptostreptococcaceae*, which houses *Clostridium difficile*, though our compositional studies did not allow for species-level resolution. It is plausible that species within the *Bacteroidaceae* family display similar competitive properties.

In summary, our current and previously reported findings show that NHE3 activity is a strong determinant of stable eubiotic gut microbiome. While the contribution of NHE3 to mucosal homeostasis is likely complex and multifactorial, despite the inherent methodological difficulties, we could demonstrate that disrupted apical Na^+/H^+ exchange contributes to the timing and severity of intestinal inflammation at least in part through modulation of the gut microbial ecology and decreased synthesis of SCFA's.

Methods

Mice

Ethics Statement—All animals used in the experiments that were carried out at the University of Arizona were handled in accordance with University of Arizona University Animal Care (UAC) guidelines and with approved IACUC protocol (Kiela). IL-10$^{-/-}$ mouse experiments were conducted in collaboration with the University of Florida, and all animals therein were handled according to an approved University of Florida IACUC protocol (Jobin).

Co-Housing Followed by Adoptive T Cell Transfer—Rag2$^{-/-}$ mice (Rag) on a 129SvEv background were either housed with Rag or NHE3xRag2$^{-/-}$ (DKO) donors at a ratio of 2:3 Rag:donors. Littermates serving as donors were not manipulated, and only existed to share living space and donate fecal matter to the experimental Rag mice (n=2 experimental mice per cage, 3 cages, n=6 per group). All mice in this experiment were female to facilitate cohousing while avoiding aggression in minimize the influence of stress. Animals were cohoused for one week prior to adoptive transfer with naïve T cells or PBS. Mice were weighed and fecal samples were collected weekly. Littermate DKO mice that died during the course of the experiment were promptly replaced by another double knockout to keep the 2:3 ratio. Experimental mice were kept for eight weeks before sacrifice.

Fecal Microbiome Transplant into Wildtype Germ-free Mice—Fecal slurries were prepared from Rag and DKO mice. Wild-type (WT) germ-free mice on C57BL/6 genetic background were orally inoculated with one of the slurries and followed for 9 weeks, with weekly fecal sample collections. At the end of 9 weeks, mice were sacrificed and fecal samples were processed for fecal microbiome analysis.

Fecal Microbiome Transplant into Germ-free Rag$^{-/-}$ Followed by Adoptive T Cell Transfer—Fecal slurries were prepared from Rag and DKO donors. Germ-free Rag1$^{-/-}$ C57BL/6 mice were inoculated with fecal slurries from Rag or DKO mice (n=6 per group). Ex-GF mice were subsequently allowed to habituate for a week before adoptive transfer with CD4$^+$CD45RB^{HI} T cells. Mice were weighed weekly, and fecal samples collected weekly. After a little over four weeks, animals were sacrificed at the request of the veterinary personnel, and tissues were processed.

Fecal Microbiome Transplant into Germ-free IL-10$^{-/-}$ Mice—These experiments were done in collaboration with the University of Florida. All animals were handled in the University of Florida gnotobiotic animal facility. Fecal samples for the creation of donor

slurries were collected and shipped frozen to Florida for fresh slurry preparation. Germ-free IL-10$^{-/-}$ mice were inoculated with either Rag or DKO slurry. Animals were weighed weekly, and fecal samples were collected at day 0, and weeks 2, 4, 5 and 7. Additional fecal samples were collected at 2, 5, and 7 weeks for Lipocalin 2 ELISA (R&D Systems, Bio-Techne Corporation, Minneapolis, MN). At 7 weeks, the experiment was completed, animals sacrificed and tissues shipped frozen to the University of Arizona for analysis.

Histology and Pathological Interpretation

Histological preparations were done by the University of Arizona University Animal Care (UAC) Pathology Services core. Pathological interpretation and inflammation scoring was performed by an experienced veterinary pathologist (D. Besselsen; UAC) blinded to the experimental design and sample group assignment. For more detail, see Supplemental Methods section.

Immunofluorescence and Cell Quantitation

Tissue sections were analyzed by immunofluorescence for Ly6B.2, CD4, and cleaved caspase 3. Slides were de-paraffinized and hydrated, followed by antigen retrieval, blocking, and staining with primary and secondary antibody. Below is a table of the antibodies/dilutions used. For greater detail, refer to the supplemental methods section.

Primary Ab	Species & Secondary	Company/Cat #	Dilution
Ly6B.2	Rat anti mouse alloantigen 1°	Biorad MCA771GT	1:1000
	647 Chicken anti Rat IgG 2°	Life Technologies A21472	1:1000
CD4	Rabbit anti mouse recombinant 1°	Abcam ab183685	1:500
	647 Goat anti rabbit 2°	Life Technologies A21246	1:400
Cleaved Caspase 3	Rabbit anti mouse mAb 1°	Cell Signaling Technologies D175	1:1000
	647 Goat anti rabbit 2°	Life Technologies A21246	1:1000

Cells were quantified using Fiji/Image J. Multiple representative images were collected from each slide at 200× magnification, and file names blinded for analysis. For Ly6B.2 and CD4, which are surface markers, single-channel (Cy5) images were counted using the multi-point tool in Fiji, using overlaid images for reference if needed. Because cleaved caspase 3 is an apoptosis marker, making cell counting ambiguous at times, we both did a cell count and additionally measured pixel intensity per field of vision, where field of vision refers to the part of the slide occupied by tissue. Analysis was also blinded for pixel intensity counts. After all images had been counted, files were unblinded and analyzed by group.

Adoptive T Cell Transfer

Adoptive transfer of naïve CD4$^+$CD45RB^{HI} T cells was carried out as described and previously performed.[26] For more detail, see Supplemental Methods section.

Fecal Microbiome Transplant

Fecal samples were collected from untreated 129SvEv Rag2$^{-/-}$ (Rag) and NHE3xRag2$^{-/-}$ (DKO) donors. Donor fecal pellets were collected at the same time from the same donors, stored at −80°C until use, and prepared fresh the day of inoculation. On the day of inoculation, fecal samples were made into a slurry of 200 mg/ml fecal matter using sterile PBS. Slurries were promptly carried down to the animal facility on ice, where they were used to inoculate recipient mice by introducing the slurries to the oral cavity and fur (200μl slurry per mouse). Germ-free animals were inoculated once.

Fecal microbial DNA extraction

Fecal samples were collected and stored at −80°C until use. DNA was extracted in 96-well format using the DNeasy PowerSoil HTP 96 Kit (Qiagen, formerly MoBio) according to the manufacturer protocol.

Mucosal DNA and RNA extraction

Mucosal DNA and RNA were isolated from colonic segments using the AllPrep DNA/RNA Mini Kit (Qiagen, cat # 80204) with a modified protocol described in more detail in the Supplemental Methods section.

Next-Generation Sequencing

The V4 fragments of 16S rRNA gene from extracted fecal and mucosal DNA were sequenced using an Illumina MiSeq platform. More detail on library construction and sequencing is provided in the Supplemental Methods section.

Bioinformatic Analysis of the Microbiome

Bioinformatic analysis of sequenced amplicons was performed using the QIIME 1.9.1 software package, a Python-based, open-source command-line package developed for the analysis of microbial datasets. PICRUSt v. 1.1.1 (Phylogenetic Investigation of Communities by Reconstruction of Unobserved States) was used to predict metagenome functional content based on the marker gene, 16S rRNA gene surveys. More detail on the bioinformatics analysis of the data is provided in the Supplemental Methods section.

Quantitative RT-PCR

Following RNA-extraction (described above), mucosal RNA from proximal and distal segments was quantified and reverse-transcribed into cDNA (Bioline, cat # BIO-65054). Quantitative real-time PCR (qRT-PCR) was performed in 10μl reactions using Bioline mastermix (cat # BIO-86005) and FAM-conjugated probes for relevant cytokines and targets (Applied Biosystems). Cq values were obtained using the LightCycler96 thermocycler (Roche) and the LightCycler96 software (version 1.1.0.1320). Raw Cq values were exported to Microsoft Excel and the gene expression changes to experimental controls, using GAPDH as the housekeeping gene.

Fecal SCFA and Lipocalin-2 detection

SCFA analyses were performed by Creative proteomics, a Division of Creative Dynamics, Inc. (Shirley, NY) using reverse phase ultra-performance liquid chromatographic (UPLC) method described in detail in the Supplemental Methods section. Lipocalin 2 was detected by ELISA (R&D Systems, Bio-Techne Corporation, Minneapolis, MN) as described in the Supplemental Methods section.

Statistical Analysis

Statistical analyses of non-microbiome data were performed using GraphPad Prism Version 7.00. Unless otherwise indicated, comparisons of two groups in which both groups passed a Shapiro-Wilke normality test were compared by two-tailed Student t-test. Those in which one or both groups did not pass a Shapiro Wilke normality test were compared by a non-parametric Mann-Whitney U-test. For comparison of three or more groups, if three or more groups passed the Shapiro-Wilke normality test, standard ANOVA was used with a Fisher LSD post hoc test. In cases where two or more groups failed a Shapiro Wilke normality test, groups were compared by non-parametric Kruskal-Wallis test with Dunn's multiple comparison's test.

Supplementary Material

Refer to Web version on PubMed Central for supplementary material.

Acknowledgments

References

1. Coskun M. Intestinal epithelium in inflammatory bowel disease. Front Med (Lausanne). 2014; 1:24. [PubMed: 25593900]

2. Ghishan FK, Kiela PR. Epithelial transport in inflammatory bowel diseases. Inflamm Bowel Dis. 2014; 20(6):1099–1109. [PubMed: 24691115]

3. Kiela PR, Xu H, Ghishan FK. Apical NA+/H+ exchangers in the mammalian gastrointestinal tract. J Physiol Pharmacol. 2006; 57(Suppl 7):51–79.

4. Gurney MA, Laubitz D, Ghishan FK, Kiela PR. Pathophysiology of Intestinal Na+/H+ exchange. Cell Mol Gastroenterol Hepatol. 2017; 3(1):27–40. [PubMed: 28090568]

5. Schultheis PJ, Clarke LL, Meneton P, Miller ML, Soleimani M, Gawenis LR, et al. Renal and intestinal absorptive defects in mice lacking the NHE3 Na+/H+ exchanger. Nat Genet. 1998; 19(3): 282–285. [PubMed: 9662405]

6. Clayburgh DR, Musch MW, Leitges M, Fu YX, Turner JR. Coordinated epithelial NHE3 inhibition and barrier dysfunction are required for TNF-mediated diarrhea in vivo. J Clin Invest. 2006; 116(10):2682–2694. [PubMed: 17016558]

7. Amin MR, Malakooti J, Sandoval R, Dudeja PK, Ramaswamy K. IFN-gamma and TNF-alpha regulate human NHE3 gene expression by modulating the Sp family transcription factors in human intestinal epithelial cell line C2BBe1. Am J Physiol Cell Physiol. 2006; 291(5):C887–896. [PubMed: 16760259]

8. Rocha F, Musch MW, Lishanskiy L, Bookstein C, Sugi K, Xie Y, et al. IFN-gamma downregulates expression of Na(+)/H(+) exchangers NHE2 and NHE3 in rat intestine and human Caco-2/bbe cells. Am J Physiol Cell Physiol. 2001; 280(5):C1224–1232. [PubMed: 11287336]

9. Barmeyer C, Harren M, Schmitz H, Heinzel-Pleines U, Mankertz J, Seidler U, et al. Mechanisms of diarrhea in the interleukin-2-deficient mouse model of colonic inflammation. Am J Physiol Gastrointest Liver Physiol. 2004; 286(2):G244–252. [PubMed: 14715519]

10. Lenzen H, Lunnemann M, Bleich A, Manns MP, Seidler U, Jorns A. Downregulation of the NHE3-binding PDZ-adaptor protein PDZK1 expression during cytokine-induced inflammation in interleukin-10-deficient mice. PLoS One. 2012; 7(7):e40657. [PubMed: 22848392]

11. Sullivan S, Alex P, Dassopoulos T, Zachos NC, Iacobuzio-Donahue C, Donowitz M, et al. Downregulation of sodium transporters and NHERF proteins in IBD patients and mouse colitis models: potential contributors to IBD-associated diarrhea. Inflamm Bowel Dis. 2009; 15(2):261–274. [PubMed: 18942765]

12. Siddique I, Hasan F, Khan I. Suppression of Na+/H+ exchanger isoform-3 in human inflammatory bowel disease: lack of reversal by 5'-aminosalicylate treatment. Scand J Gastroenterol. 2009; 44(1):56–64. [PubMed: 18785066]

13. Yeruva S, Farkas K, Hubricht J, Rode K, Riederer B, Bachmann O, et al. Preserved Na(+)/H(+) exchanger isoform 3 expression and localization, but decreased NHE3 function indicate regulatory sodium transport defect in ulcerative colitis. Inflamm Bowel Dis. 2010; 16(7):1149–1161. [PubMed: 20027604]

14. Farkas K, Yeruva S, Rakonczay Z Jr, Ludolph L, Molnar T, Nagy F, et al. New therapeutic targets in ulcerative colitis: the importance of ion transporters in the human colon. Inflamm Bowel Dis. 2011; 17(4):884–898. [PubMed: 20722063]

15. Subramanya SB, Rajendran VM, Srinivasan P, Nanda Kumar NS, Ramakrishna BS, Binder HJ. Differential regulation of cholera toxin-inhibited Na-H exchange isoforms by butyrate in rat ileum. Am J Physiol Gastrointest Liver Physiol. 2007; 293(4):G857–863. [PubMed: 17690171]

16. Hayashi H, Szaszi K, Coady-Osberg N, Furuya W, Bretscher AP, Orlowski J, et al. Inhibition and redistribution of NHE3, the apical Na+/H+ exchanger, by Clostridium difficile toxin B. J Gen Physiol. 2004; 123(5):491–504. [PubMed: 15078917]

17. Hodges K, Alto NM, Ramaswamy K, Dudeja PK, Hecht G. The enteropathogenic Escherichia coli effector protein EspF decreases sodium hydrogen exchanger 3 activity. Cell Microbiol. 2008; 10(8):1735–1745. [PubMed: 18433466]

18. Ambort D, Johansson ME, Gustafsson JK, Nilsson HE, Ermund A, Johansson BR, et al. Calcium and pH-dependent packing and release of the gel-forming MUC2 mucin. Proc Natl Acad Sci U S A. 2012; 109(15):5645–5650. [PubMed: 22451922]

19. Johansson ME, Gustafsson JK, Holmen-Larsson J, Jabbar KS, Xia L, Xu H, et al. Bacteria penetrate the normally impenetrable inner colon mucus layer in both murine colitis models and patients with ulcerative colitis. Gut. 2014; 63(2):281–291. [PubMed: 23426893]

20. Laubitz D, Larmonier CB, Bai A, Midura-Kiela MT, Lipko MA, Thurston RD, et al. Colonic gene expression profile in NHE3-deficient mice: evidence for spontaneous distal colitis. Am J Physiol Gastrointest Liver Physiol. 2008; 295(1):G63–G77. [PubMed: 18467500]

21. Kiela PR, Laubitz D, Larmonier CB, Midura-Kiela MT, Lipko MA, Janikashvili N, et al. Changes in mucosal homeostasis predispose NHE3 knockout mice to increased susceptibility to DSS-induced epithelial injury. Gastroenterology. 2009; 137(3):965–975. 975 e961–910. [PubMed: 19450596]

22. Larmonier CB, Laubitz D, Hill FM, Shehab KW, Lipinski L, Midura-Kiela MT, et al. Reduced colonic microbial diversity is associated with colitis in NHE3-deficient mice. Am J Physiol Gastrointest Liver Physiol. 2013; 305(10):G667–677. [PubMed: 24029465]

23. Engevik MA, Aihara E, Montrose MH, Shull GE, Hassett DJ, Worrell RT. Loss of NHE3 alters gut microbiota composition and influences Bacteroides thetaiotaomicron growth. Am J Physiol Gastrointest Liver Physiol. 2013; 305(10):G697–711. [PubMed: 24072680]

24. Bloom SM, Bijanki VN, Nava GM, Sun L, Malvin NP, Donermeyer DL, et al. Commensal Bacteroides species induce colitis in host-genotype-specific fashion in a mouse model of inflammatory bowel disease. Cell Host Microbe. 2011; 9(5):390–403. [PubMed: 21575910]

25. Hansen JJ, Huang Y, Peterson DA, Goeser L, Fan TJ, Chang EB, et al. The colitis-associated transcriptional profile of commensal Bacteroides thetaiotaomicron enhances adaptive immune responses to a bacterial antigen. PLoS One. 2012; 7(8):e42645. [PubMed: 22880065]

26. Laubitz D, Harrison CA, Midura-Kiela MT, Ramalingam R, Larmonier CB, Chase JH, et al. Reduced Epithelial Na+/H+ Exchange Drives Gut Microbial Dysbiosis and Promotes Inflammatory Response in T Cell-Mediated Murine Colitis. PLoS One. 2016; 11(4):e0152044. [PubMed: 27050757]

27. Du Z, Hudcovic T, Mrazek J, Kozakova H, Srutkova D, Schwarzer M, et al. Development of gut inflammation in mice colonized with mucosa-associated bacteria from patients with ulcerative colitis. Gut Pathog. 2015; 7:32. [PubMed: 26697117]

28. Garrett WS, Lord GM, Punit S, Lugo-Villarino G, Mazmanian SK, Ito S, et al. Communicable ulcerative colitis induced by T-bet deficiency in the innate immune system. Cell. 2007; 131(1):33–45. [PubMed: 17923086]

29. Soave O, Brand CD. Coprophagy in animals: a review. Cornell Vet. 1991; 81(4):357–364. [PubMed: 1954740]

30. Laukens D, Brinkman BM, Raes J, De Vos M, Vandenabeele P. Heterogeneity of the gut microbiome in mice: guidelines for optimizing experimental design. FEMS Microbiol Rev. 2016; 40(1):117–132. [PubMed: 26323480]

31. Sellon RK, Tonkonogy S, Schultz M, Dieleman LA, Grenther W, Balish E, et al. Resident enteric bacteria are necessary for development of spontaneous colitis and immune system activation in interleukin-10-deficient mice. Infect Immun. 1998; 66(11):5224–5231. [PubMed: 9784526]

32. Chassaing B, Srinivasan G, Delgado MA, Young AN, Gewirtz AT, Vijay-Kumar M. Fecal lipocalin 2, a sensitive and broadly dynamic non-invasive biomarker for intestinal inflammation. PLoS One. 2012; 7(9):e44328. [PubMed: 22957064]

33. Buisson A, Vazeille E, Minet-Quinard R, Goutte M, Bouvier D, Goutorbe F, et al. Fecal Matrix Metalloprotease-9 and Lipocalin-2 as Biomarkers in Detecting Endoscopic Activity in Patients With Inflammatory Bowel Diseases. J Clin Gastroenterol. 2017

34. Li X, Cai L, Xu H, Geng C, Lu J, Tao L, et al. Somatostatin regulates NHE8 protein expression via the ERK1/2 MAPK pathway in DSS-induced colitis mice. Am J Physiol Gastrointest Liver Physiol. 2016; 311(5):G954–G963. [PubMed: 27686614]

35. Yeruva S, Chodisetti G, Luo M, Chen M, Cinar A, Ludolph L, et al. Evidence for a causal link between adaptor protein PDZK1 downregulation and Na(+)/H(+) exchanger NHE3 dysfunction in human and murine colitis. Pflugers Arch. 2015; 467(8):1795–1807. [PubMed: 25271043]

36. Janecke AR, Heinz-Erian P, Muller T. Congenital Sodium Diarrhea: A Form of Intractable Diarrhea, With a Link to Inflammatory Bowel Disease. J Pediatr Gastroenterol Nutr. 2016; 63(2):170–176. [PubMed: 26835907]

37. Pryde SE, Duncan SH, Hold GL, Stewart CS, Flint HJ. The microbiology of butyrate formation in the human colon. FEMS Microbiol Lett. 2002; 217(2):133–139. [PubMed: 12480096]

38. Van den Abbeele P, Belzer C, Goossens M, Kleerebezem M, De Vos WM, Thas O, et al. Butyrate-producing Clostridium cluster XIVa species specifically colonize mucins in an in vitro gut model. ISME J. 2013; 7(5):949–961. [PubMed: 23235287]

39. Johansson ME, Larsson JM, Hansson GC. The two mucus layers of colon are organized by the MUC2 mucin, whereas the outer layer is a legislator of host-microbial interactions. Proc Natl Acad Sci U S A. 2011; 108(Suppl 1):4659–4665. [PubMed: 20615996]

40. Johansson ME, Phillipson M, Petersson J, Velcich A, Holm L, Hansson GC. The inner of the two Muc2 mucin-dependent mucus layers in colon is devoid of bacteria. Proc Natl Acad Sci U S A. 2008; 105(39):15064–15069. [PubMed: 18806221]

41. Walker AW, Duncan SH, McWilliam Leitch EC, Child MW, Flint HJ. pH and peptide supply can radically alter bacterial populations and short-chain fatty acid ratios within microbial communities from the human colon. Appl Environ Microbiol. 2005; 71(7):3692–3700. [PubMed: 16000778]

42. Kiela PR, Kuscuoglu N, Midura AJ, Midura-Kiela MT, Larmonier CB, Lipko M, et al. Molecular mechanism of rat NHE3 gene promoter regulation by sodium butyrate. Am J Physiol Cell Physiol. 2007; 293(1):C64–74. [PubMed: 17344314]

43. Musch MW, Bookstein C, Xie Y, Sellin JH, Chang EB. SCFA increase intestinal Na absorption by induction of NHE3 in rat colon and human intestinal C2/bbe cells. Am J Physiol Gastrointest Liver Physiol. 2001; 280(4):G687–693. [PubMed: 11254495]

44. Couturier-Maillard A, Secher T, Rehman A, Normand S, De Arcangelis A, Haesler R, et al. NOD2-mediated dysbiosis predisposes mice to transmissible colitis and colorectal cancer. J Clin Invest. 2013; 123(2):700–711. [PubMed: 23281400]

45. Berry D, Kuzyk O, Rauch I, Heider S, Schwab C, Hainzl E, et al. Intestinal Microbiota Signatures Associated with Inflammation History in Mice Experiencing Recurring Colitis. Front Microbiol. 2015; 6:1408. [PubMed: 26697002]

46. Engevik MA, Engevik KA, Yacyshyn MB, Wang J, Hassett DJ, Darien B, et al. Human Clostridium difficile infection: inhibition of NHE3 and microbiota profile. Am J Physiol Gastrointest Liver Physiol. 2015; 308(6):G497–509. [PubMed: 25552580]

47. Reeves AE, Koenigsknecht MJ, Bergin IL, Young VB. Suppression of Clostridium difficile in the gastrointestinal tracts of germfree mice inoculated with a murine isolate from the family Lachnospiraceae. Infect Immun. 2012; 80(11):3786–3794. [PubMed: 22890996]
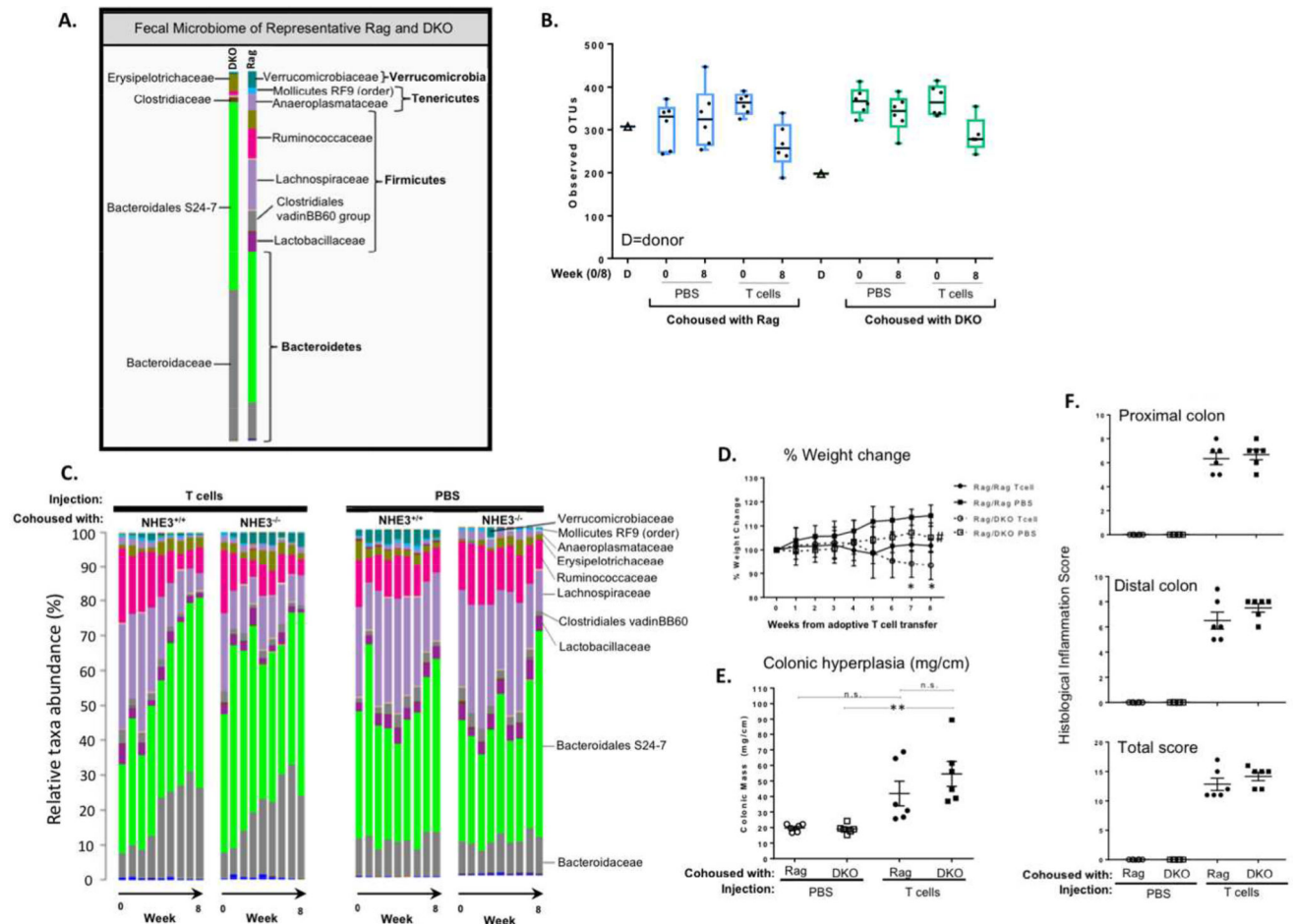
Figure 1. Passive microbiome sharing (cohousing) is inefficient and does not confer susceptibility to colitis

Rag mice were cohoused with either other Rag2$^{-/-}$ or DKO (NHE3xRag2$^{-/-}$ double knockout) littermates in a 2:3 ratio Rag:donor. Rag mice (2 per cage, 6 per group) were adoptively transferred with 0.5×10^5 naïve CD4$^+$CD45RB^{hi} T cells or injected with sterile PBS (control). Fecal samples were collected weekly for microbiome analysis. **A**. A family level microbiome composition for Rag and DKO fecal donors as a reference. **B**. Alpha diversity analysis depicting observed OTUs between Rag or DKO fecal donors (D=donor) and in co-housed Rag mice either adoptively transferred with naive T cells or injected with PBS. **C**. Family-level taxonomic composition at weekly time points in Rag mice co-housed with NHE3$^{+/+}$ Rag mice or with NHE3$^{-/-}$ Rag mice, with adoptive T cell transfer or injected with PBS. **D**. Percent weight change, measured weekly, among recipient Rag mice. T cell-transferred Rag mice cohoused with DKO mice lost more weight than those co-housed with DKO (*). Among PBS-injected Rag mice, those co-housed with DKO mice tended to have lower body weight than those co-housed with Rag mice (#) (two-way ANOVA). **E**. Colonic hyperplasia of Rag mice as measured weight/length ratio at sacrifice. **F**. Histological inflammation score as measured by a pathologist blinded to experimental design.
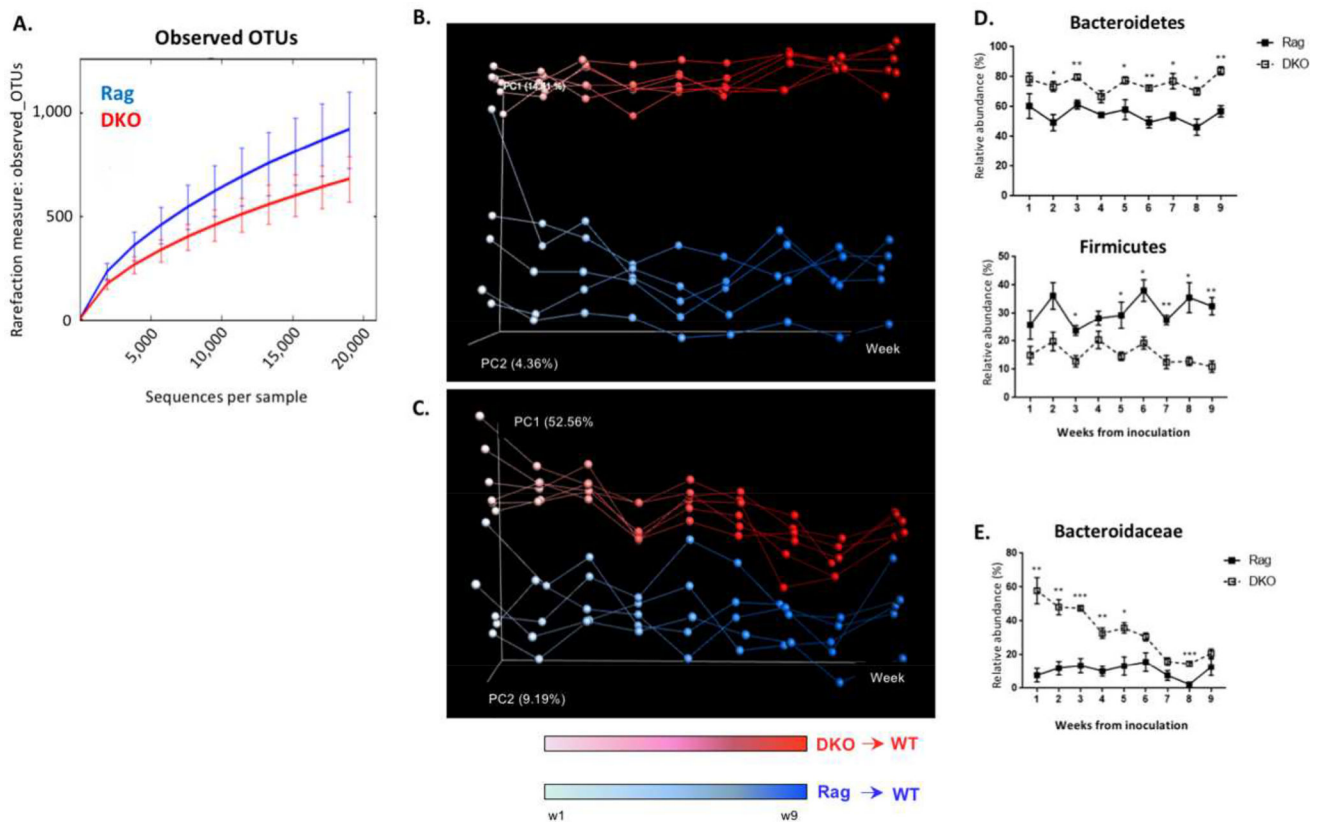
Figure 2. NHE3$^{+/+}$ and NHE3$^{-/-}$ microbiomes are stably transferrable to germ-free WT recipients

Fecal microbiome transplant (FMT) from Rag (NHE3$^{+/+}$) or DKO (NHE3xRag2$^{-/-}$ double knockout) mice into wildtype germ-free mice. Mice were maintained for nine weeks post-colonization with weekly fecal collections (w1 to w9). **A**. Alpha rarefaction plot depicting observed OTUs from wildtype mice that had received FMT from either Rag (blue) or DKO (red) donors. **B**. Principal coordinate analysis depicting beta diversity over time in an unweighted UNIFRAC analysis. **C**. Principal coordinate analysis depicting the beta diversity over time in a weighted UNIFRAC analysis, which takes into account the abundance of each taxa in its calculation. **D**. Relative abundance (% of total) of *Bacteroidetes* and *Firmicutes* in GF wildtype mice inoculated with Rag or DKO microbiota. **E.** Relative abundance (% of total) of *Bacteroidaceae* family over time in GF wildtype mice inoculated with Rag or DKO microbiota. * p<0.05, ** p<0.01, *** p<0.001. Two-Way ANOVA.
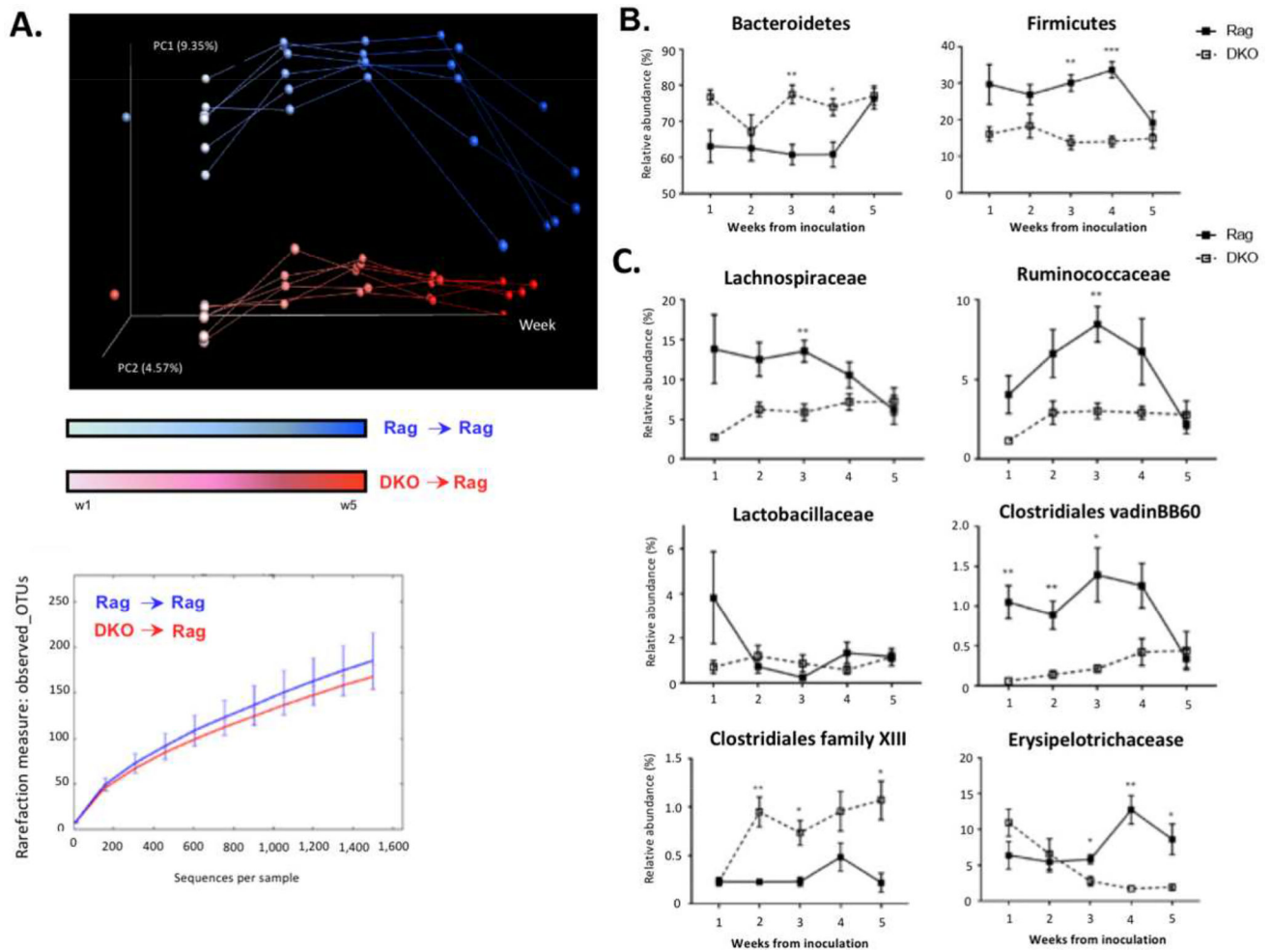
Figure 3. Convergence of microbiomes of the FMT recipients during inflammation in adoptive T cell transfer

Germ-free Rag mice were colonized with microbiome from either Rag or DKO (NHE3xRag2$^{-/-}$) mice. All mice were adoptively transferred with 0.5×10^5 naïve CD4$^+$CD45RB^{hi} T cells 7 days later. Time points (weekly) are shown in reference to the time of inoculation. **A**. (Upper panel) Principal coordinate analysis depicting beta diversity (unweighted UNIFRAC) over time in Rag recipients of Rag or DKO FMT. Single, unconnected blue and red dots represent the Rag and DKO donors, respectively; (lower panel) alpha rarefaction plot depicting the alpha diversity shown as observed OTUs in Rag recipients of FMT from either Rag (blue) or DKO (red) fecal donors **B**. relative abundance of the two main bacterial phyla, *Bacteroidetes* and *Firmicutes* among the two FMT groups. **C**. Relative abundance of selected families among Rag recipients of FMT from either Rag or DKO donors. * p<0.05, ** p<0.01, *** p<0.001. Two-Way ANOVA.
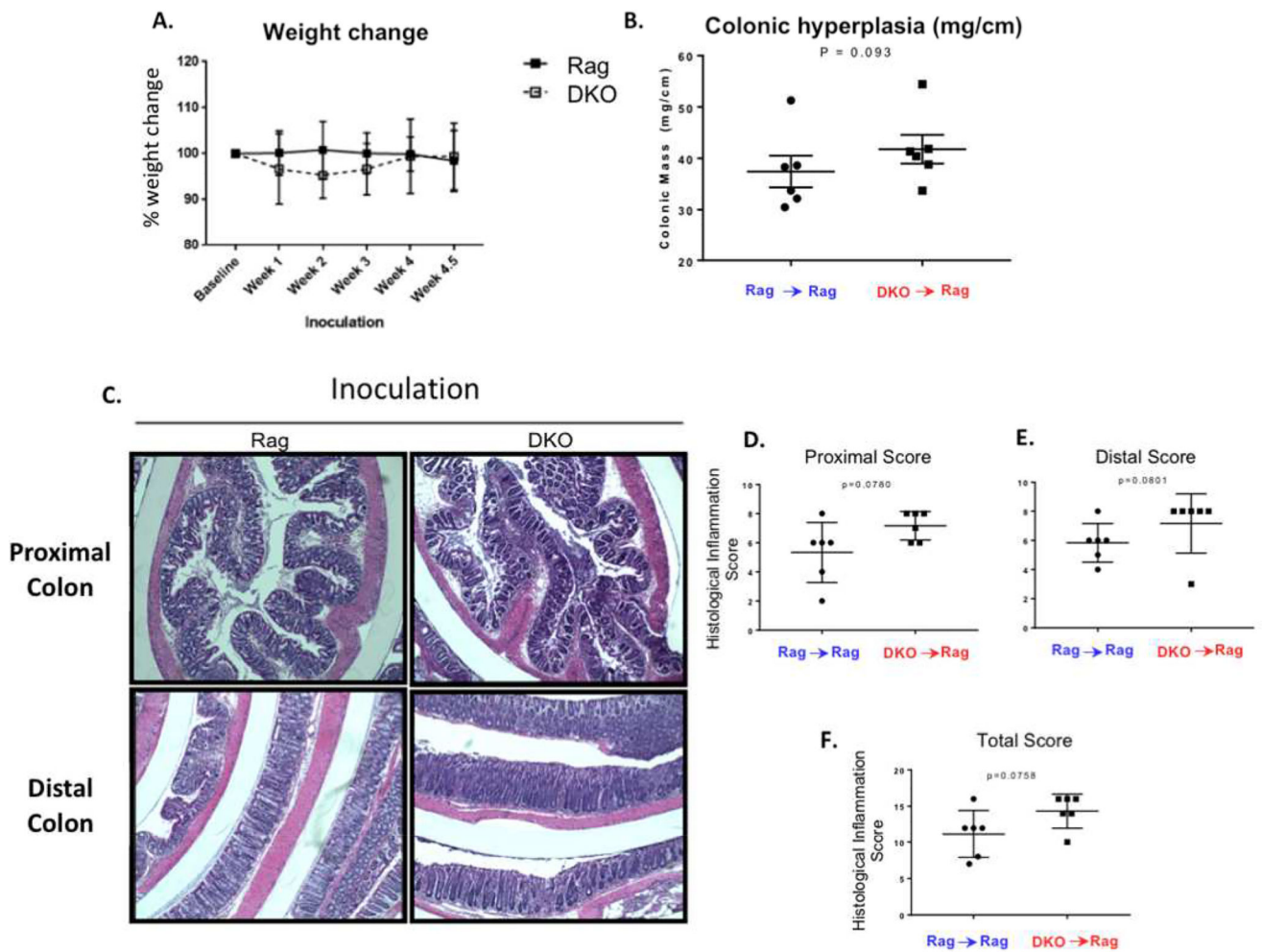
Figure 4. Microbiota convergence diminishes the differences in inflammatory response to adoptive T cell transfer in ex-GF Rag mice

A. Relative body weight loss, measured weekly, in Rag recipients of Rag or DKO (NHE3xRag2$^{-/-}$) FMT after adoptive T cell transfer. **B**. Colonic hyperplasia in Rag recipients of the respective FMT, expressed as mg/cm of the colon at sacrifice. **C**. Representative H&E stained proximal and distal colonic sections from Rag recipients of FMT (100× magnification). **D**. Proximal, **E**. distal, and **F**. combined histological inflammation scores.
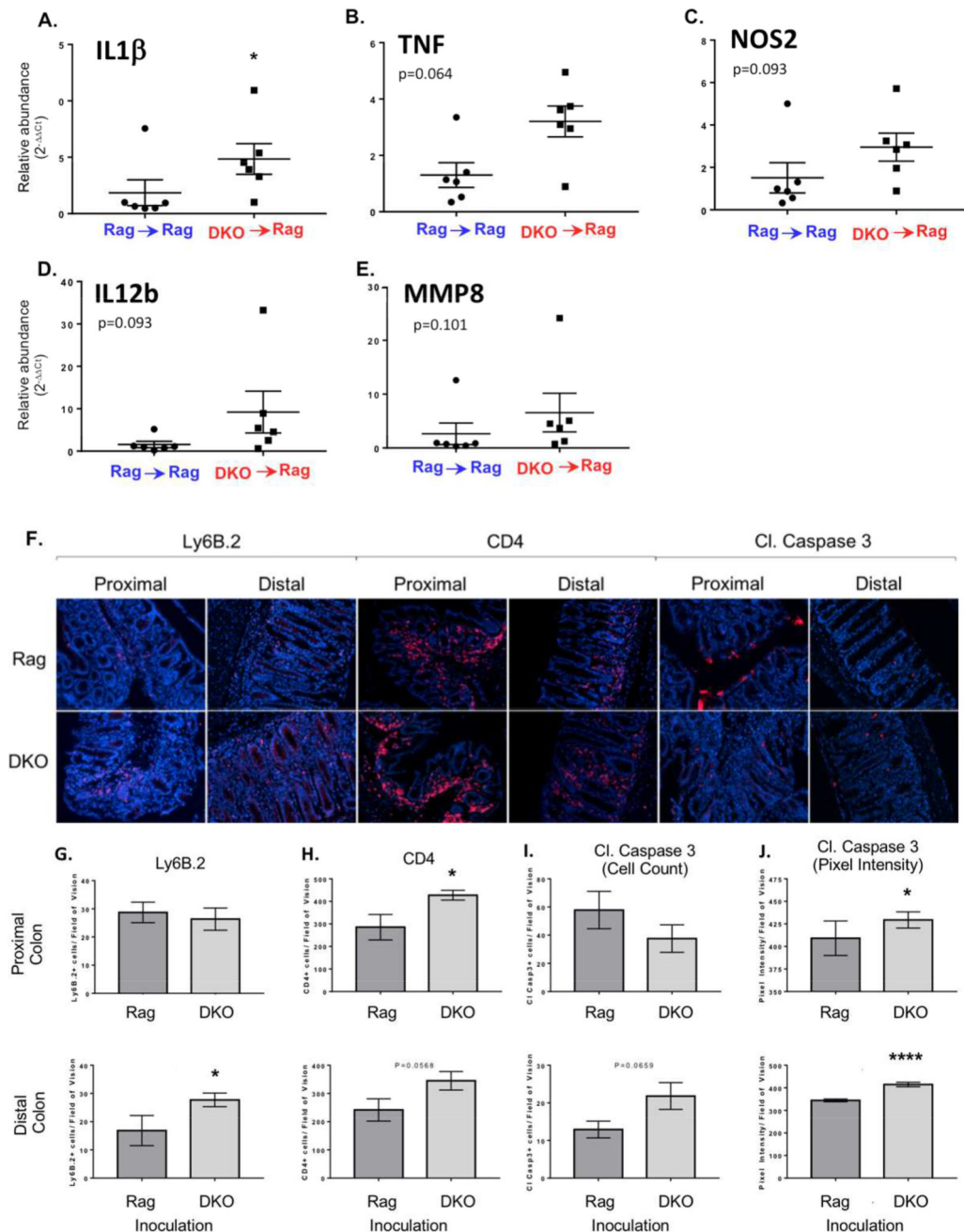
Figure 5. Increased cytokine expression and immune infiltration in the recipients of DKO FMT after adoptive naïve T cell transfer

A–E. RT-qPCR assessment of colonic expression of selected inflammatory mediators. Data analyzed by Student T-test, p values indicated in graph. **F.** Immunofluorescence imaging of Ly6B.2$^+$, CD4$^+$, and cleaved caspase 3$^+$ cells as seen in proximal and distal colonic sections (200× magnification). **G–I.** Quantitation of Ly6B.2$^+$, CD4$^+$, and cleaved caspase 3$^+$ cells by colonic segment as counted in Image J by blinded analysis. **J**. Pixel intensity per field of vision for cleaved caspase 3, as an apoptotic marker, calculated by Image J in a blinded analysis. **G–J**. * p<0.05, ** p<0.01, *** p<0.001, **** p<0.0001.
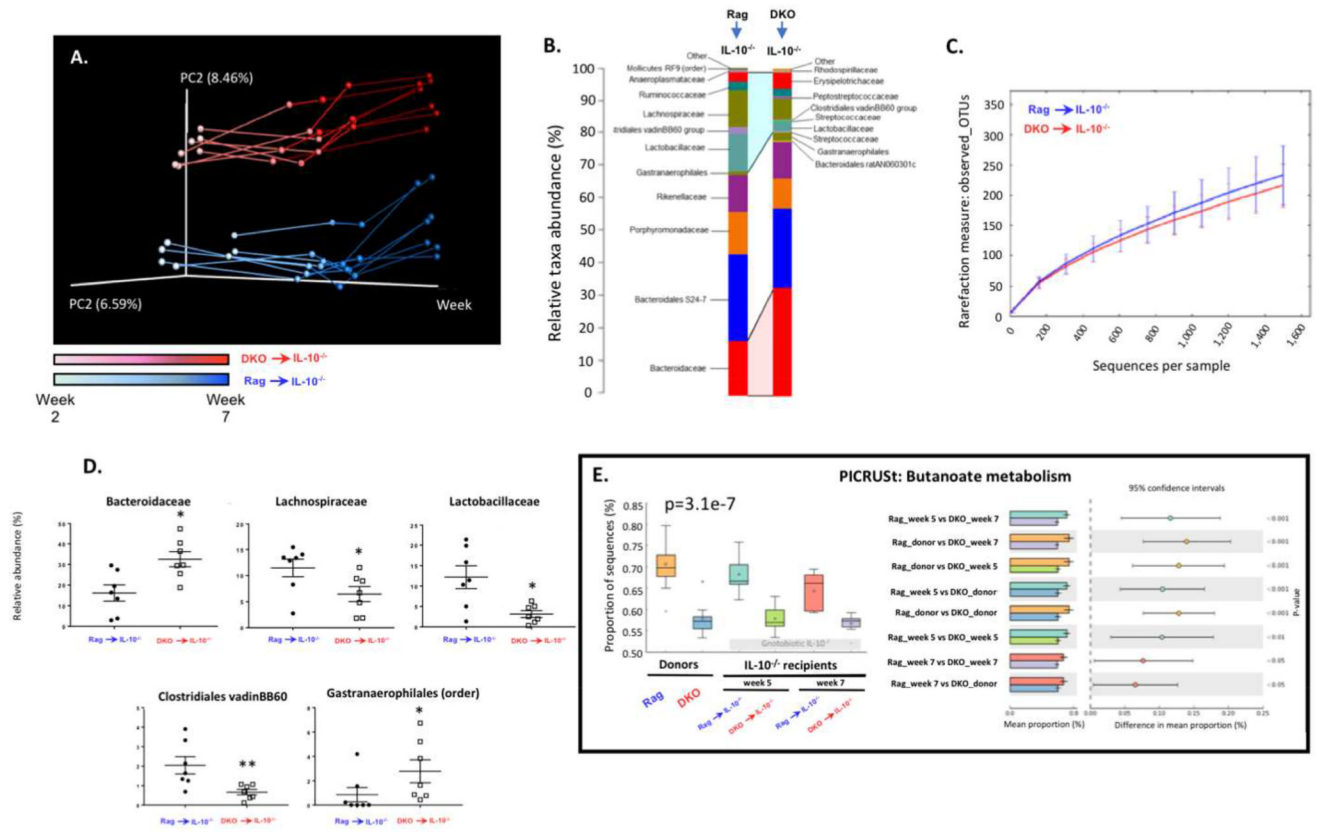
Figure 6. Fecal microbiota of germ-free IL-10$^{-/-}$ mice colonized with microbial community from Rag of DKO mice remain stably different over time

GF IL-10$^{-/-}$ mice were colonized with fecal microbiome from either Rag or DKO (NHE3xRag2$^{-/-}$) donors and maintained for seven weeks, with prospective fecal collection. **A.** Principal coordinate analysis showing beta diversity over time (unweighted UNIFRAC) in IL-10$^{-/-}$ recipients of FMT from Rag (blue) or DKO (red) mice. **B.** Family-level microbiome composition bar charts depicting the fecal microbiomes at sacrifice in IL-10$^{-/-}$ recipients of Rag (Rag → IL-10$^{-/-}$) or DKO (DKO → IL-10$^{-/-}$) microbiome. **C.** Alpha-rarefaction plot depicting alpha diversity shown in observed OTUs of the fecal microbiome between IL-10$^{-/-}$ recipients of Rag (blue) or DKO (red) FMT. **D.** Relative abundance of selected bacterial families from IL-10$^{-/-}$ recipients of FMT measured at sacrifice (week 7). * p<0.05, ** p<0.01, Mann-Whitney U-test. **E.** Ontology category related to butyric acid metabolism identified by PICRUSt prediction of functional profiling of the microbial communities based on the 16S rRNA gene sequences. P value of box plots indicate the result of Kruskal-Wallis H-test. Extended error bar plots to the right indicate pairwise comparison among groups with p value * p<0.05 (pairwise comparison using Tukey-Kramer post-hoc test).
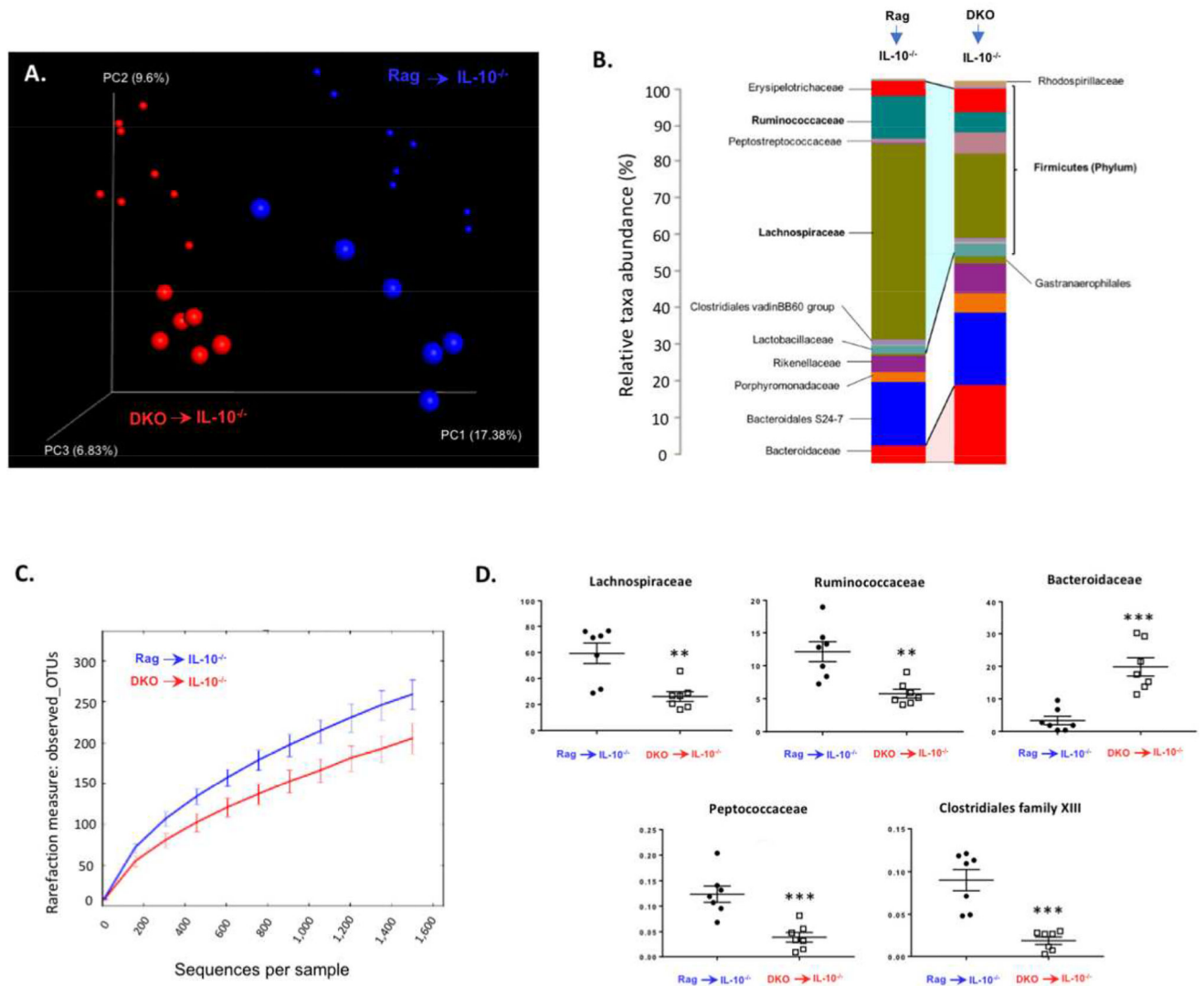
Figure 7. Mucosa-associated microbiome of ex-GF IL-10$^{-/-}$ mice colonized with fecal microbiome from NHE3-deficient mice shows significant reductions in protective taxa

Proximal and distal colonic segments were resected from IL-10$^{-/-}$ mice that had received FMT from either Rag (NHE3$^{+/+}$) or DKO (NHE3xRag2$^{-/-}$) mice. DNA was extracted from colonic segments and the bacterial 16S DNA sequenced to determine the composition of the mucosa-associated microbiome. Data from the proximal colon, the more affected segment in the IL-10-deficiency model, is presented. **A.** Principal coordinate analysis demonstrating beta diversity (unweighted UNIFRAC) of the mucosal microbiome at sacrifice between IL-10$^{-/-}$ recipients of Rag (NHE3$^{+/+}$, blue) or DKO (NHE3xRag2$^{-/-}$, red) FMT. Larger dots represent males, smaller dots represent females. **B.** Family-level microbiome composition of IL-10$^{-/-}$ recipients of FMT from Rag or DKO mice. **C.** Rarefaction plot depicting alpha diversity (observed OTUs) in ex-GF IL-10$^{-/-}$ mice. **D.** Relative abundance of selected bacterial families in the proximal colonic mucosa of ex-GF IL-10$^{-/-}$ mice that had received FMT from either Rag or DKO donors. * p<0.05, ** p<0.01, *** p<0.001.
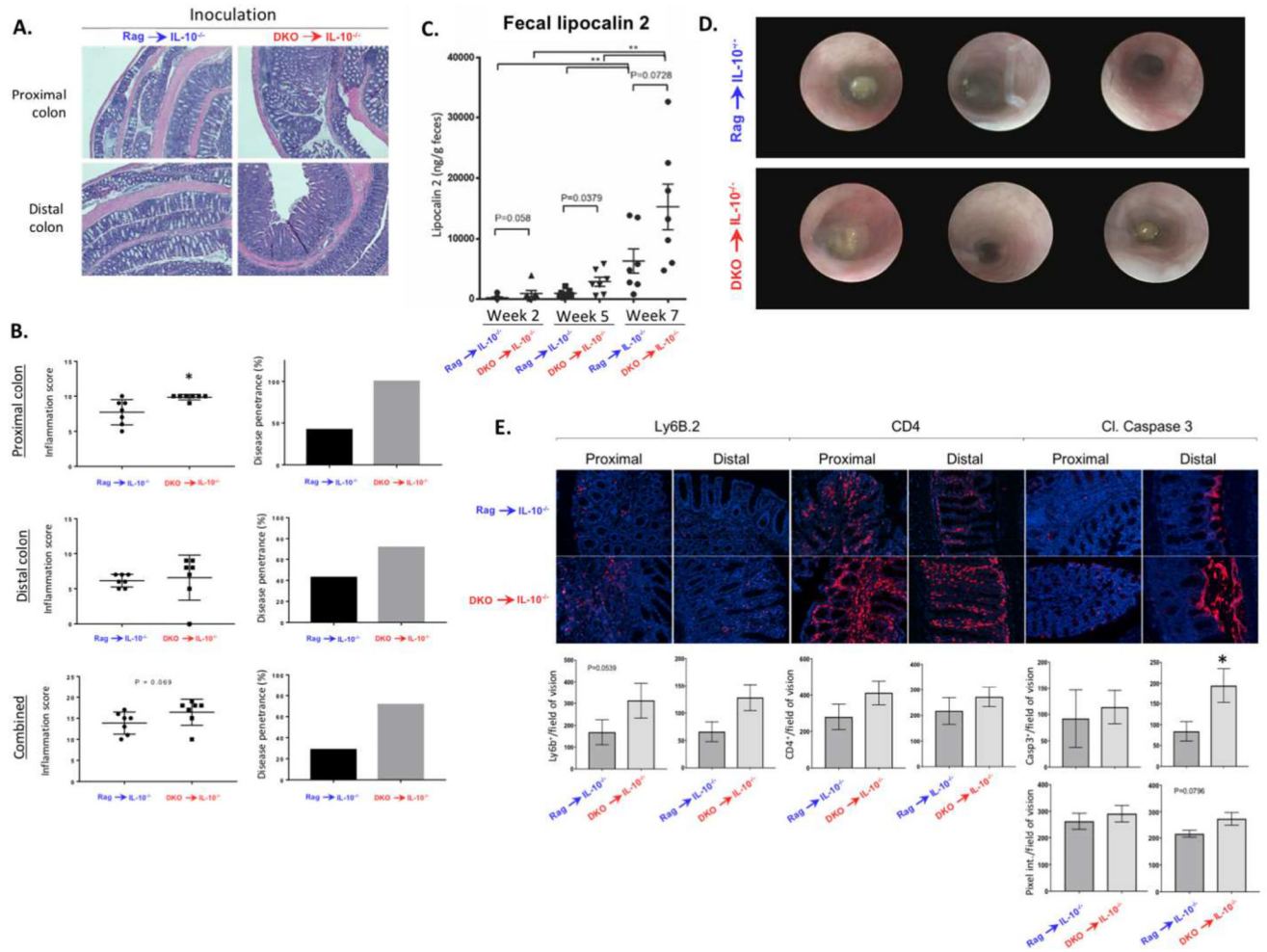
Figure 8. Colonization of GF IL-10$^{-/-}$ mice with fecal microbiome from NHE3$^{-/-}$ donors accelerates the onset and severity of colitis in IL-10$^{-/-}$ mice

A. Representative H&E-stained sections from ex-GF IL-10$^{-/-}$ mice colonized with microbiomes from Rag or DKO (NHE3xRag2$^{-/-}$) mice. **B.** Histological inflammation scores in the proximal and distal colon, the composite total score, and the penetrance of disease calculated by the fraction of animals that had a higher histological inflammation score than the median score of the control (IL-10$^{-/-}$ colonized with Rag microbiome) group. **C.** ELISA analysis lipocalin 2 concentration in fecal samples collected at 2, 5, and 7 weeks post-colonization. P values indicated (Mann-Whitney U-test). **D.** Representative colonoscopy images captured at the 5-week time point, depicting colonic mucosa of ex-GF IL-10$^{-/-}$ mice colonized with microbiomes from either Rag (top panel) or DKO mice (bottom panel). **E.** Immunofluorescence imaging of Ly6B.2^{+}, CD4^{+}, and cleaved caspase 3^{+} cells as seen in proximal and distal colonic sections (200× magnification); quantitation of Ly6B.2^{+}, CD4^{+}, and cleaved caspase 3^{+} cells by colonic segment. For cleaved caspase 3, pixel intensity per field of vision is also calculated (* p<0.05).